AGU PUBLICATIONS

JGR

Journal of Geophysical Research: Solid Earth

RESEARCH ARTICLE
10.1002/2016JB013387

Analyzing paleomagnetic data: To anchor or not to anchor?

David Heslop[1] and Andrew P. Roberts[1]

[1]Research School of Earth Sciences, Australian National University, Canberra, ACT, Australia

Key Points:
- The effect of anchoring principal component fits to paleomagnetic demagnetization data is investigated
- Anchoring elongates the covariance structure of demagnetization data in a manner that is difficult to justify from a statistical standpoint
- We provide a new constrained principal component technique that avoids the issues associated with anchoring

Correspondence to:
D. Heslop,
david.heslop@anu.edu.au

Citation:
Heslop, D., and A. P. Roberts (2016), Analyzing paleomagnetic data: To anchor or not to anchor?, *J. Geophys. Res. Solid Earth*, *121*, 7742–7753, doi:10.1002/2016JB013387.

Received 21 JUL 2016
Accepted 26 OCT 2016
Accepted article online 1 NOV 2016
Published online 14 NOV 2016

Abstract Paleomagnetic directions provide the basis for use of paleomagnetism in chronological and tectonic reconstructions and for constraining past geomagnetic field behavior over a variety of timescales. Crucial to paleomagnetic analysis is the separation and quantification of a characteristic remanent magnetization (ChRM), which relates to a process of interest, from other remanence components. Principal component analysis (PCA) of stepwise demagnetization data is employed routinely in these situations to estimate magnetic remanence directions and their uncertainties. A given ChRM is often assumed to trend toward the origin of a vector demagnetization diagram and prevailing data analysis frameworks allow remanence directions to be estimated based on PCA fits that are forced to pass through the origin of such diagrams, a process referred to as "anchoring." While this approach is adopted commonly, little attention has been paid to the effects of anchoring and the influence it has on both estimated remanence directions and their associated uncertainties. In almost all cases, anchoring produces an artificially low uncertainty estimation compared to an unanchored fit. Bayesian model selection demonstrates that the effects of anchoring cannot typically be justified from a statistical standpoint. We present an alternative to anchoring that constrains the best fit remanence direction to pass through the origin of a vector demagnetization diagram without unreasonably distorting the representation of the demagnetization data.

1. Introduction

Magnetic remanences preserved in rocks and sediments provide the basis for paleomagnetic reconstructions. The natural remanent magnetization (NRM) of a paleomagnetic specimen may, however, contain several components that were acquired at different times during the geological history of the sampled rock unit [*Irving*, 1964; *McElhinny*, 1973; *Tarling*, 1983]. To isolate the characteristic remanent magnetization (ChRM), which often corresponds to the remanence direction acquired during formation of the rock, it is necessary to magnetically "clean" the NRM to remove any additional remanence components [*As and Zijderveld*, 1958; *Collinson et al.*, 1967]. Cleaning is achieved via a process of stepwise demagnetization, whereby the NRM is progressively randomized with the aim of gradually isolating the ChRM. The need for stepwise demagnetization to identify all remanence components in a specimen is now accepted universally in paleomagnetism.

Stepwise demagnetization data are readily visualized using a vector demagnetization diagram, where distinct remanence components appear as straight line segments [*Zijderveld*, 1967; *Dunlop*, 1979]. The paleomagnetic direction associated with any given remanence component can be estimated by performing principal component analysis (PCA) on the data within the associated range of demagnetization steps and by determining the direction of the leading principal component [*Kirschvink*, 1980]. Often, the ChRM is isolated when all additional remanence components have been removed; therefore, the data that define the ChRM should trend toward the origin of a vector demagnetization diagram. This property is employed as key selection criteria when interpreting vector demagnetization diagrams; if a demagnetization segment does not trend toward the origin of the diagram, then it implies that multiple remanence components are present. *Kirschvink* [1980] showed that in the case of a hypothesized ChRM component, the PCA solution that represents the corresponding demagnetization segment can be forced to pass through the origin of the vector demagnetization diagram. This process is termed "anchoring" and is attractive from a theoretical standpoint because the PCA solution can be constrained to obey the behavior expected for many ChRM components.

As part of the PCA framework for analyzing demagnetization data, *Kirschvink* [1980] proposed use of the maximum angular deviation (MAD) to represent the directional uncertainty associated with a given remanence component. MAD is typically employed as a selection criterion for rejecting specimens with scattered demagnetization data. There are no generally accepted MAD cutoffs for specimen rejection; however, a remanence

segment yielding MAD > 15° would be treated as questionable, while MAD < 10° would be considered to be reasonably good [*McElhinny and McFadden*, 2000]. Studies requiring high-quality paleomagnetic directions from which to draw robust inferences concerning the paleomagnetic field have sometimes employed an acceptance/rejection cutoff of MAD < 5° [*Johnson et al.*, 1998]. MAD values are also often plotted as a function of depth in paleomagnetic studies of long sediment cores to illustrate how data quality varies through different depth intervals [e.g., *Channell et al.*, 2013].

Scatter in demagnetization data can be attributed to multiple sources, such as the random walk nature of stepwise demagnetization and instrument noise [*Khokhlov and Hulot*, 2016]. For scattered data it becomes necessary for an investigator to determine if a hypothesized ChRM trends toward the origin and, thus, if the use of an anchored fit is potentially appropriate. The decision to anchor a fit is usually made by visual inspection, i.e., does the demagnetization segment trend toward the origin? Determining whether data trend toward the origin of a vector demagnetization diagram is, however, more complicated than it may appear at face value. It is not sufficient for points projected onto the orthogonal planes of a vector demagnetization diagram to appear to be directed toward the origin. They represent the same vector and must, therefore, intercept the origin of the plot at the same point. In many cases this requirement is difficult to assess visually.

MAD-based criteria have been developed to determine if demagnetization data trend toward the origin. For example, the Deviation ANGle (DANG) compares the MAD to the angle between the unanchored paleomagnetic component and the direction between the mean of the demagnetization data and the origin [*Pick and Tauxe*, 1993; *Tauxe and Staudigel*, 2004]. If the DANG is less than the MAD, then it is assumed that the component trends toward the origin. It is important to note, however, that the DANG is based on the MAD of an unanchored PCA solution and does not consider fully changes to the PCA fit induced by anchoring. Anchoring will change both the direction and uncertainty associated with a PCA solution, and it is essential to assess if this change can be justified given the data. Existing metrics, such as DANG, do not address this question and, therefore, cannot be used as direct justification for adopting an anchored fit.

Recently, *Heslop and Roberts* [2016] developed a Bayesian framework to quantify the directional uncertainty in isolated remanence components. In a similar vein, here we address the question of how the anchoring process changes a traditional PCA [*Kirschvink*, 1980] fit, in terms of both estimated direction and uncertainty, and show how key data processing decisions can be addressed in a rigorous and statistically justified manner. We adopt a simple Bayesian model selection technique that provides an estimate of the probability that the data support the use of an anchored rather than an unanchored PCA solution. This information can, therefore, be used to make a statistically informed decision as to whether anchoring should be employed or not. Such evidence-based decisions are crucial if higher-order paleomagnetic statistics, such as site mean directions, are to be calculated in a rigorous manner that optimizes the amount of paleomagnetic information that can be extracted from a measured data set. Finally, we propose a new form of constrained fit through the origin of a vector demagnetization diagram, which appears to overcome a number of the shortcomings of traditional PCA anchoring.

2. Principal Component Analysis

Analysis of stepwise demagnetization data requires identification of univectorial segments that may carry geomagnetic or geological information [*Zijderveld*, 1967; *Dunlop*, 1979]. The magnetization (M), inclination (I), and declination (D) of a segment of N demagnetization data considered to represent a univectorial trend can be represented as follows in a Cartesian coordinate system:

$$t_1(i) = M(i)\cos I(i)\cos D(i), \tag{1}$$

$$t_2(i) = M(i)\cos I(i)\sin D(i), \tag{2}$$

and

$$t_3(i) = M(i)\sin I(i), \tag{3}$$

where i is the ith demagnetization point and the mean of the segment is

$$\bar{\mathbf{t}} = \frac{1}{N}\sum_{i=1}^{N}\mathbf{t}(i). \tag{4}$$

A covariance matrix can then be defined as follows:

$$\mathbf{S} = \begin{pmatrix} \sum \delta t_1(i)\delta t_1(i) & \sum \delta t_1(i)\delta t_2(i) & \sum \delta t_1(i)\delta t_3(i) \\ \sum \delta t_2(i)\delta t_1(i) & \sum \delta t_2(i)\delta t_2(i) & \sum \delta t_2(i)\delta t_3(i) \\ \sum \delta t_3(i)\delta t_1(i) & \sum \delta t_3(i)\delta t_2(i) & \sum \delta t_3(i)\delta t_3(i) \end{pmatrix} /N, \tag{5}$$

where

$$\delta\mathbf{t}(i) = \mathbf{t}(i) - \bar{\mathbf{t}}. \tag{6}$$

S is more readily expressed in matrix form as follows:

$$\mathbf{S} = (\mathbf{t} - \bar{\mathbf{t}})^T(\mathbf{t} - \bar{\mathbf{t}})/N, \tag{7}$$

where ^{T} represents the matrix transpose. The direction of the best fit vector (in a least squares sense) through the data is determined by solving:

$$\mathbf{S}\mathbf{u}_i = \lambda_i \mathbf{u}_i, \qquad i = 1, \ldots, 3, \tag{8}$$

where the eigenvectors and eigenvalues of **S** are denoted by $\mathbf{u}_i$ and λ_i, respectively. The eigenvalues and eigenvectors are then reordered so that $\lambda_1 \geq \lambda_2 \geq \lambda_3$. The inclination and declination of the leading eigenvector, $\mathbf{u}^*$, (normalized to unit length) are as follows:

$$I = \arcsin\left(\mathbf{u}_3^*\right), \tag{9}$$

and

$$D = \arctan\left(\mathbf{u}_2^*/\mathbf{u}_1^*\right). \tag{10}$$

For univectorial demagnetization, data deviations from the fitted vector are represented by the second and third eigenvectors; however, such deviations are expected to be minor (i.e., $\lambda_1 \gg \lambda_2 \simeq \lambda_3$). Under this assumption, the MAD [*Kirschvink*, 1980] is the conical angle between the leading eigenvector and the minor cross section of the prolate ellipsoid defined by the eigenvalues:

$$\mathrm{MAD} = \arctan\left(\sqrt{\frac{\lambda_2 + \lambda_3}{\lambda_1}}\right). \tag{11}$$

As discussed above, if a demagnetization segment trends toward the origin of the vector demagnetization diagram, it may be considered to be a ChRM that warrants an anchored fit constrained to pass through the origin. This constraint can be imposed by assuming that the mean of the demagnetization segment coincides with the origin [*Kirschvink*, 1980], yielding a covariance matrix:

$$\mathbf{S_A} = \begin{pmatrix} \sum t_1(i)t_1(i) & \sum t_1(i)t_2(i) & \sum t_1(i)t_3(i) \\ \sum t_2(i)t_1(i) & \sum t_2(i)t_2(i) & \sum t_2(i)t_3(i) \\ \sum t_3(i)t_1(i) & \sum t_3(i)t_2(i) & \sum t_3(i)t_3(i) \end{pmatrix} /N \tag{12}$$

that represents a mixture of the data covariance and mean, which can be represented in matrix form as follows:

$$\mathbf{S_A} = (\mathbf{t} - \bar{\mathbf{t}})^T(\mathbf{t} - \bar{\mathbf{t}})/N + \bar{\mathbf{t}}^T\bar{\mathbf{t}}. \tag{13}$$

Replacing **S** with $\mathbf{S_A}$ in equation (8) provides the direction and MAD of the anchored fit ($\mathrm{MAD_A}$). PCA in this form has served the paleomagnetic community for over 35 years.

3. Quantifying the Effect of Anchoring

The matrix forms of **S** (equation (7)) and $\mathbf{S_A}$ (equation (13)) provide an accessible representation to understand the effects of anchoring paleomagnetic data. It is apparent that anchored directions and $\mathrm{MAD_A}$ depend on both the data mean and covariance. Consider an isotropic three-dimensional Gaussian distribution with a standard deviation of σ and, therefore, a covariance matrix; $\sigma^2\mathbf{I}$, where **I** is a 3-by-3 identity matrix.

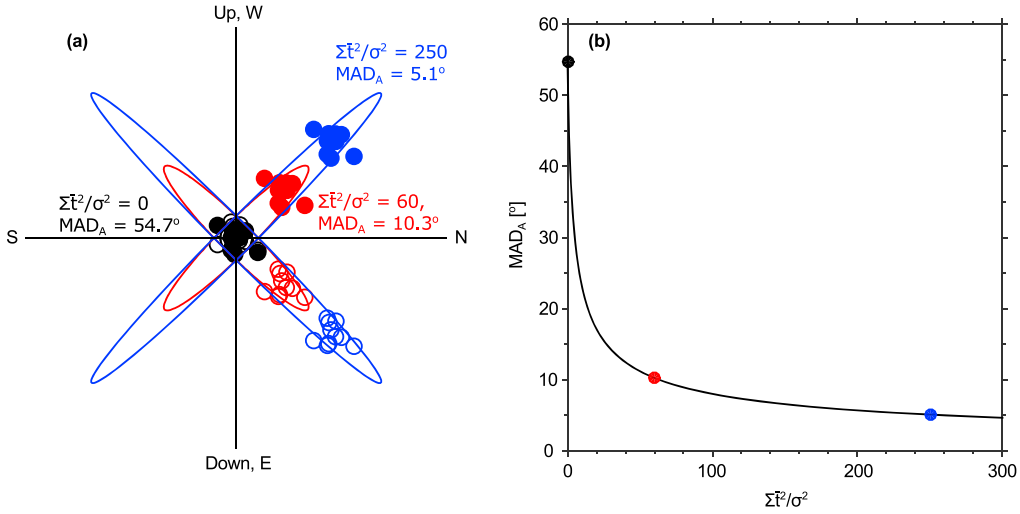

Figure 1. (a) Illustration of the dependance of the maximum angular deviation of an anchored PCA fit (MAD_A) on the relative magnitudes of the mean and covariance of an isotropic Gaussian distribution. As the magnitude of the mean ($\sum \bar{\mathbf{t}}^2$) increases with respect to the distribution variance (σ^2), the anchored covariance structures (ellipses) become more elongated, and MAD_A is reduced. (b) MAD_A as a function of $\sum \bar{\mathbf{t}}^2$ and σ^2. This simple example is for isotropic data, which is not typical in paleomagnetism, but demonstrates that when considering demagnetization data the relative magnitudes of the remanence segment mean and covariance will both exert control over MAD_A. In contrast, MAD depends only on the data covariance (i.e., it is independent of the mean). The colored points in Figure 1b correspond to the specific examples in Figure 1a.

This distribution has no preferred direction, so its eigenvalues are simply $\lambda_1 = \lambda_2 = \lambda_3 = \sigma^2$, which according to equation (11) corresponds to MAD = arctan $\sqrt{2}$ = 54.7°. The rightmost term of $\mathbf{S_A}$ (equation (13)) represents the contribution of the mean to an anchored PCA fit. The matrix $\bar{\mathbf{t}}^T\bar{\mathbf{t}}$ has a rank of 1, with $\lambda_1 = \sum \bar{\mathbf{t}}^2$ and $\lambda_2 = \lambda_3 = 0$. Therefore, in the simple isotropic case, when the contributions from the data mean and covariance are brought together in $\mathbf{S_A}$, the eigenvalues are $\lambda_1 = \sum \bar{\mathbf{t}}^2 + \sigma^2$ and $\lambda_2 = \lambda_3 = \sigma^2$. This system is illustrated in Figure 1a, where an example isotropic data set is migrated away from the origin of a vector demagnetization plot. As the magnitude of the data mean increases with respect to the data covariance, the ellipsoid representing $\mathbf{S_A}$ becomes more elongated and MAD_A decreases. For the specific case of an isotropic Gaussian distribution, MAD_A can be calculated as a function of the magnitude of the distribution mean with respect to the distribution covariance (Figure 1b).

An example using simulated data with a preferred direction is given in Figure 2, where ellipses are drawn to represent unanchored and anchored covariance structures. In the unanchored case (Figure 2a), the data segment appears to trend toward the origin of the vector demagnetization diagram and the PCA fit yields a MAD of 7.5°. Visual inspection of the data trajectory suggests that it could intercept the origin of the vector demagnetization diagram, which is supported by a DANG (2.4°) less than the MAD. In the case of an anchored solution, it is apparent that the anchoring process has dramatically elongated the covariance matrix (Figure 2b), which yields a MAD_A of 2.5°. In this example the decision to anchor the fit changes the estimated direction to an extent that is consistent with the DANG statistic, but the MAD-based directional uncertainty is reduced by a factor of 3. This effect could cause confusion in terms of MAD-based specimen selection criteria. The high unanchored MAD would imply that the corresponding paleomagnetic direction should be treated with caution or that the specimen should be rejected. In contrast, MAD_A is small enough that the anchored paleomagnetic direction may be considered to be of high quality; however, the reduced uncertainty is purely an artifact of the anchoring process. Thus, when deciding whether a fit should be anchored, it is not enough to consider solely the effect on the direction, but it is also crucial to consider the effect on the associated directional uncertainty. To address this question, we employed Bayes' theorem to estimate the extent to which the data favor the use of an anchored rather than an unanchored PCA fit. To achieve this, traditional PCA needs to be placed in a probabilistic framework, which provides a representation to compare unanchored and anchored models directly.

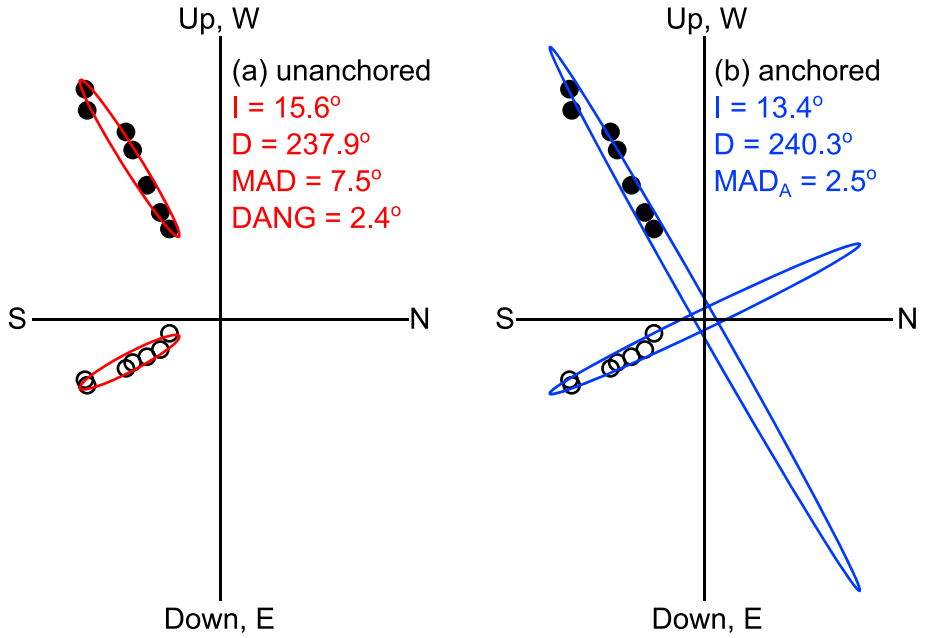

Figure 2. Comparison of covariance structures (colored ellipses) employed in (a) unanchored and (b) anchored principal component analysis (PCA) fits to the example data (open and filled circles represent vertical and horizontal components, respectively). In this example, the DANG suggests that the data trend to the origin; however, elongation in the $\mathbf{S_A}$ covariance structure induced by anchoring reduces the MAD-based uncertainty for the estimated anchored direction by a factor of 3. Thus, the decision to anchor the PCA solution has a dramatic effect on the apparent uncertainty of the resulting paleomagnetic direction.

3.1. Probabilistic Principal Component Analysis

Tipping and Bishop [1999] provided a probabilistic PCA model (PPCA), whereby data are represented as realizations from a multivariate Gaussian distribution that accounts for both signal and noise contributions. *Heslop and Roberts* [2016] showed how PPCA can be employed in analyzing demagnetization segments, whereby perfect univectorial data will fall on a line in three-dimensional space, the direction of which can be represented by $\mathbf{W}$, which is a three-element vector with covariance matrix $\mathbf{W}^T\mathbf{W}$. In combination with the segment mean, $\boldsymbol{\mu}$, such univectorial behavior can be represented probabilistically by the three-dimensional Gaussian distribution; $\mathcal{N}(\boldsymbol{\mu}, \mathbf{W}^T\mathbf{W})$. Deviations from perfect univectorial behavior, whether as a result of measurement noise or random walk behavior during demagnetization [*Khokhlov and Hulot*, 2016], are considered to be realizations from an isotropic Gaussian distribution with a standard deviation of σ, i.e., $\mathcal{N}(0, \sigma^2\mathbf{I})$, where $\mathbf{I}$ is a 3-by-3 identity matrix. Combining the two Gaussian distributions that represent the signal and deviations results in a further Gaussian distribution [*Tipping and Bishop*, 1999]:

$$\mathbf{t} \sim \mathcal{N}(\boldsymbol{\mu}, \mathbf{C}), \tag{14}$$

where $\mathbf{C} = \mathbf{W}^T\mathbf{W} + \sigma^2\mathbf{I}$. This approach provides a probabilistic formulation to represent univectorial demagnetization data. The maximum likelihood estimate of $\boldsymbol{\mu}$ is the data mean given by $\bar{\mathbf{t}}$ in section 2, while maximum likelihood estimates of $\mathbf{W}$ and σ^2 can be calculated directly in the three-dimensional case from the PCA solution derived in section 2:

$$\sigma^2 = \frac{\lambda_2 + \lambda_3}{2}, \tag{15}$$

and

$$\mathbf{W} = \mathbf{u}^* \sqrt{\lambda_1 - \sigma^2}. \tag{16}$$

Referring back to equation (11), the MAD can also be calculated for the maximum likelihood model as follows:

$$\mathrm{MAD} = \arctan\left(\sqrt{\frac{2\sigma^2}{\lambda_1}}\right). \tag{17}$$

Table 1. Grades of Statistical Support Corresponding to Different $p(H_A|D)$ Values When Comparing Unanchored and Anchored Fits Defined by H_U and H_A, Respectively (Based on *Raftery* [1995]).

$p(H_A\|D)$	Evidence
<0.01	Unanchored: very strong support
0.01 to <0.05	Unanchored: strong support
0.05 to <0.25	Unanchored: positive support
0.25 to <0.50	Unanchored: weak support
0.50	No preference
>0.50 to <0.75	Anchored: weak support
0.75 to <0.95	Anchored: positive support
0.95 to <0.99	Anchored: strong support
≥0.99	Anchored: very strong support

Given the covariance matrix (**S** or $\mathbf{S_A}$ for the unanchored and anchored fits, respectively), the model log likelihood is given by the following:

$$\log \mathcal{L} = -\frac{N}{2}\{3\ln(2\pi) + \ln|\mathbf{C}| + \mathrm{tr}(\mathbf{C}^{-1}\mathbf{S})\}, \tag{18}$$

where $|\mathbf{C}|$ is the determinant of **C** and tr is the matrix trace. The ability to calculate the model likelihood and estimate the maximum likelihood parameters provides a means to develop a procedure to determine the support provided by demagnetization data for use of an anchored PCA model.

3.2. Bayesian Model Selection

The aim of Bayesian model selection techniques is to estimate the probabilities of different models based on available data. In the case of demagnetization data, two models (written in terms of hypotheses) must be considered.

1. H_U: The demagnetization data are realizations drawn from a Gaussian distribution $\mathcal{N}(\boldsymbol{\mu}, \mathbf{C})$, where **C** is based on the unanchored PPCA solution.
2. H_A: The demagnetization data are realizations drawn from a Gaussian distribution $\mathcal{N}(0, \mathbf{C})$, where **C** is based on the anchored PPCA solution.

The probability that a specific hypothesis, H, is correct given the observed data (i.e., $p(H|D)$) is estimated by Bayes' theorem [*Bayes*, 1763]:

$$p(H|D) = \frac{p(D|H)p(H)}{p(D)}, \tag{19}$$

where $p(D|H)$ is the probability of observing the data given H, $p(H)$ is the a priori probability that H is correct, and $p(D)$ is the probability of observing the data independently of any specific hypothesis. If H_U and H_A are combined, it is possible to cancel $p(D)$:

$$\frac{p(H_U|D)}{p(H_A|D)} = \frac{p(D|H_U)}{p(D|H_A)} \cdot \frac{p(H_U)}{p(H_A)}, \tag{20}$$

where the left-hand term is the posterior odds, which represents the relative strength of the evidence for H_U and H_A. If the two hypotheses are deemed a priori to be equally probable (i.e., $p(H_U) = p(H_A) = 0.5$), the last term of equation (20) cancels, and the first term on the right of equation (20), which is known as the Bayes factor (BF), gives the posterior odds.

Estimation of BF can be challenging. *Wagenmakers* [2007] developed a simplified method to estimate an approximate BF based on the Bayesian information criterion (BIC) of *Schwarz* [1978]. For a given hypothesis, H, given the data, D, the BIC of the maximum likelihood model is given by the following:

$$\mathrm{BIC} = -2\log\mathcal{L} + k\ln(N), \tag{21}$$

where k is the number of unknowns in the model. Unanchored PPCA is based on eight unknowns (three unknowns in μ, three unknowns in $\mathbf{u}^*$, plus λ_1 and σ^2), whereas anchored PPCA treats μ as a known (the origin);

thus, there are five unknowns remaining. The approximate Bayes factor is then given by [*Masson*, 2011] the following:

$$\mathrm{BF} = \frac{p(D|H_U)}{p(D|H_A)} \approx \exp\left((\mathrm{BIC}(H_A) - \mathrm{BIC}(H_U))/2\right). \tag{22}$$

Using this approximation for BF, the posterior probability that the data favor H_U (unanchored model) is as follows:

$$p(H_U|D) = \frac{\mathrm{BF}}{\mathrm{BF}+1}. \tag{23}$$

The system is limited to two hypotheses, so the posterior probability that the data favor H_A (anchored model) is as follows:

$$p(H_A|D) = 1 - p(H_U|D). \tag{24}$$

The BIC-based approximation of BF is expected to provide a somewhat conservative estimate of the support for H_A [*Raftery*, 1999]. This effect helps to protect against incorrectly selecting an anchored PCA fit and is not considered detrimental to the proposed approach.

Use of an anchored fit can only be justified if $p(H_A|D)$ (a probability between 0 and 1) is sufficiently high. It is important to recognize that this is a model selection procedure, and we do not propose that arbitrary cutoffs are chosen to decide whether a solution should be anchored or not. Instead, anchored fits should be quoted with $\mathrm{MAD_A}$ and $p(H_A|D)$ values. *Jeffreys* [1961] and *Raftery* [1995] provided descriptive rules for interpreting Bayes factors, which can be written in terms of $p(H_A|D)$ to assign an accepted term describing the strength of the evidence supporting H_A (Table 1). These descriptions respect the continuous nature of $p(H_A|D)$ and purposely avoid the hard binary decision of assigning one model as "right" and the other as "wrong."

3.3. Real Examples

To illustrate the proposed technique, a number of examples based on data from *Johnson et al.* [1998] are given to demonstrate the use of $p(H_A|D)$. *Johnson et al.* [1998] studied lavas from São Miguel Island (Azores) from which we provide examples from their stepwise thermal and alternating field demagnetization experiments. It is important to note that the chosen examples were selected to illustrate our proposed technique, and we do not question the analysis or conclusions of *Johnson et al.* [1998] who did not anchor any of their PCA fits. For specimen az13b2 (Figure 3a), anchoring has little effect on the estimated direction, but the MAD is reduced by ~35% and $p(H_A|D) = 0.52$, which corresponds to *weak* support for the anchored model (which is consistent with the DANG, which indicates that the data trend toward the origin). Similarly, a slight deviation in the anchored direction of specimen az23a1 (Figure 3b) from the unanchored fit and a reduction in the associated MAD by a third yields $p(H_A|D) = 0.17$, which implies that there is *positive* support in favor of an unanchored fit. Thus, even though the DANG implies that the data trend toward the origin, anchoring is not supported statistically. Anchoring of specimen az26j2 (Figure 3c) causes a change in the estimated direction of $> 6°$, the MAD is reduced from 12.1° to 6.3° and $p(H_A|D) = 0.01$, which corresponds to *strong* support for an unanchored fit. Finally, specimen az12e1 (Figure 3d) yields $p(H_A|D) = 0.00$ (*very strong* support for an unanchored fit), which results from large changes in both the fitted direction and MAD (consistent with DANG).

To experienced paleomagnetists the results of the analysis in Figure 3 may appear surprising. Typically, demagnetization data that appear to be directed toward the origin are taken to provide empirical support for an anchored fit. As demonstrated by our model selection analysis, however, the form of $\mathbf{S_A}$ makes it difficult to justify an anchored fit from a statistically rigorous standpoint even for a remanence component that is clearly directed toward the origin (e.g., Figure 3b). Even if the directions that result from unanchored and anchored fits are the same, often, the reduction in MAD resulting from anchoring cannot be justified within a probabilistic framework. As demonstrated in Figure 1, this effect becomes more pronounced the farther the centroid of the demagnetization data is away from the origin.

The presented Bayesian analysis does not discount the possibility that a remanence direction determined from a PCA solution should be forced to pass through the origin, but rather that the current technique of assuming $\mathcal{N}(0, \mathbf{C})$ is a statistically inappropriate means to impose this constraint. Instead, it is necessary to develop a technique that constrains the fitted vector to pass through the origin while distorting the representation of the covariance structure as little as possible.

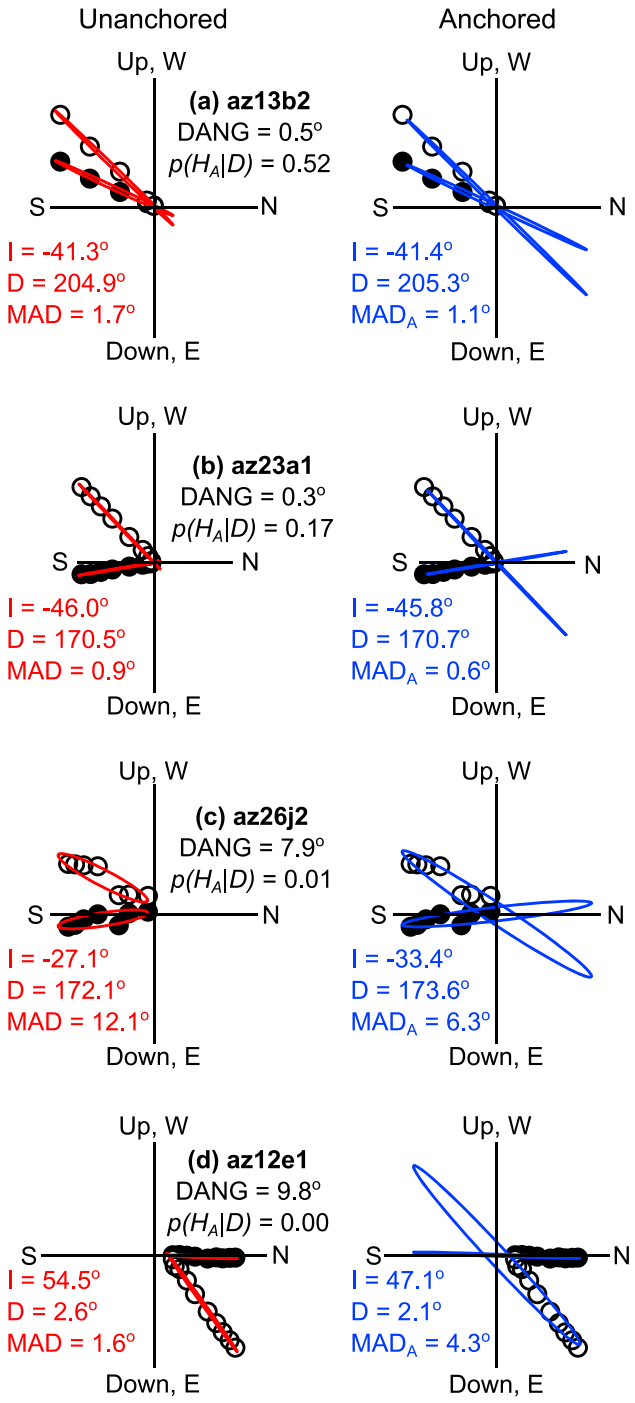

Figure 3. Examples of stepwise demagnetization data from *Johnson et al.* [1998] with a variety of MAD and DANG values. Representations of the covariance structures of the unanchored and anchored fits are shown in red and blue, respectively. The DANG values suggest that the demagnetization data from specimens (a) az13b2, (b) az23a1, and (c) az26j2 trend toward the origin and could potentially be anchored, but this is not supported by $p(H_A|D)$, which suggests that only specimen az13b2 should be anchored (*weak* support). This lack of support for anchoring results from the elongation induced in the model covariance structure by the anchoring process. (d) For specimen az12e1, both DANG and $p(H_A|D)$ suggest that an anchored fit is inappropriate.

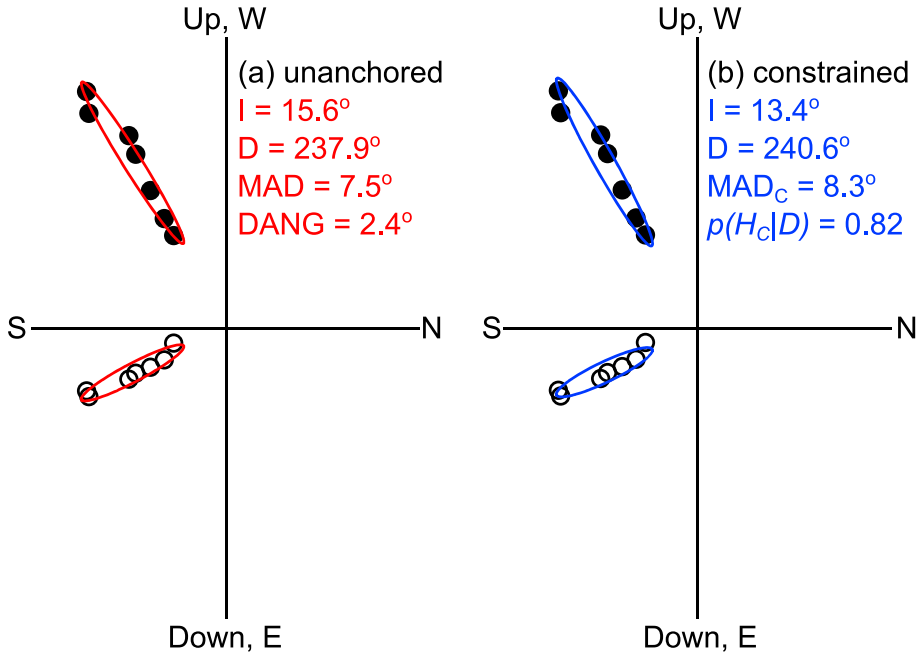

Figure 4. Comparison of covariance structures (colored ellipses) employed in (a) unanchored and (b) constrained PPCA fits calculated from the same example data shown in Figure 2 (scaling is the same as in Figure 2, with open and filled circles representing vertical and horizontal components, respectively). While anchoring induces an elongation in the covariance structure that is not supported statistically ($p(H_A|D) = 0.001$), the constrained fit still passes through the origin and causes minimal distortion to the covariance and, thus, receives positive statistical support; $p(H_C|D) = 0.82$.

4. Constrained PPCA

Building on the PPCA model of *Tipping and Bishop* [1999], a maximum likelihood fit needs to be sought that is constrained to pass through the origin of a vector demagnetization diagram. The PPCA model (equation (14)) lends itself readily to such a constraint. By definition, the leading principal component must pass through the mean of the data, the maximum likelihood estimate of which is $\bar{\mathbf{t}}$. If the leading principal component passes through the mean of the data and is constrained to pass through the origin, then its direction is given by the unit vector $\bar{\mathbf{t}}/\|\bar{\mathbf{t}}\|$. This yields a constrained version of $\mathbf{W}$:

$$\mathbf{W_C} = \frac{\bar{\mathbf{t}}}{\|\bar{\mathbf{t}}\|}\sqrt{\lambda_C - \sigma_C^2}. \tag{25}$$

Table 2. Grades of Statistical Support Corresponding to Different $p(H_C|D)$ Values When Comparing Unanchored and Constrained Fits Defined by H_U and H_C, Respectively (Based on *Raftery* [1995])

$p(H_C\|D)$	Evidence
<0.01	Unanchored: very strong support
0.01 to <0.05	Unanchored: strong support
0.05 to <0.25	Unanchored: positive support
0.25 to <0.50	Unanchored: weak support
0.50	No preference
>0.50 to <0.75	Constrained: weak support
0.75 to <0.95	Constrained: positive support
0.95 to <0.99	Constrained: strong support
≥0.99	Constrained: very strong support

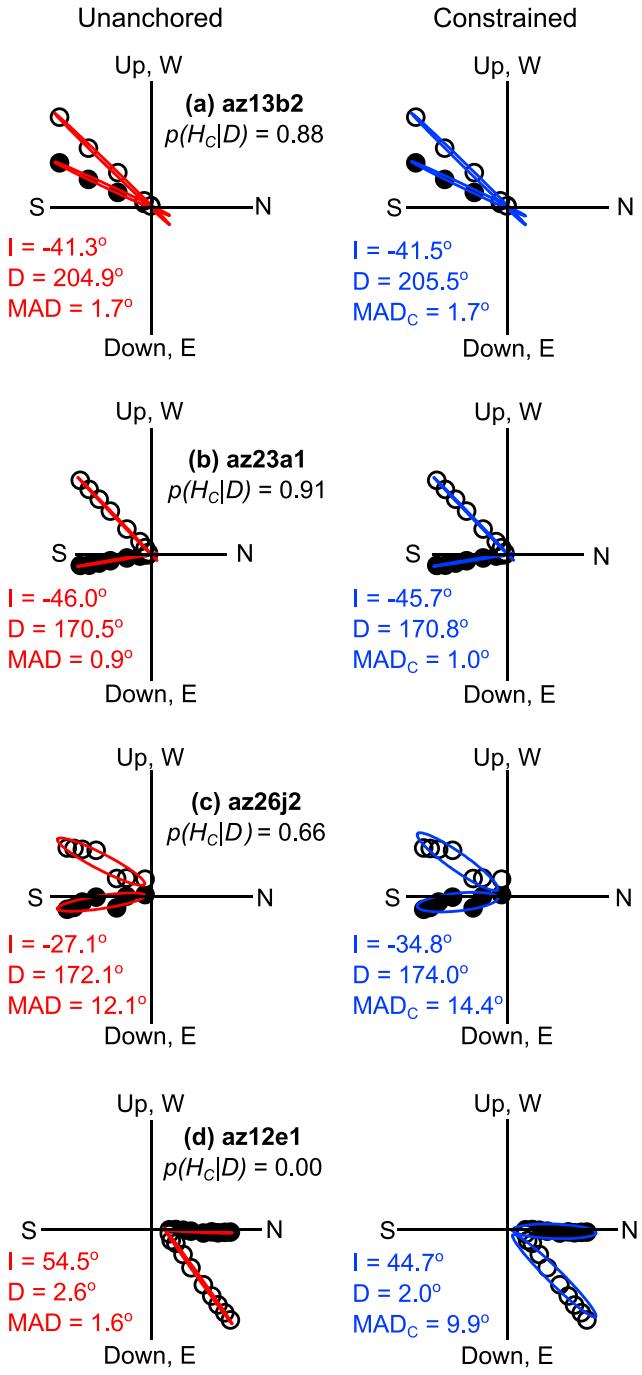

Figure 5. Examples of stepwise demagnetization data from *Johnson et al.* [1998] (same specimens as Figure 3). Constrained PPCA produces vectors that pass through the origin, but without spuriously elongated covariance structures. The constrained fits cause little distortion to the covariance structures of specimens (a) az13b2 and (b) az23a1, which receive positive statistical support. For (c) specimen az26j2, the constrained fit has weak statistical support. In contrast, the covariance structure of the constrained fit to specimen (d) az12e1 requires a greater broadening to accommodate a fit through the origin. This broadening results in a greatly increased MAD_C and cannot be supported statistically, with very strong support for an unanchored fit.

Based on equation (18), the log likelihood is given by the following:

$$\log \mathcal{L} = -\frac{N}{2}\left\{3\ln(2\pi) + \ln|\mathbf{C_C}| + \mathrm{tr}\left(\mathbf{C_C}^{-1}\mathbf{S}\right)\right\}, \tag{26}$$

where given the definition of $\mathbf{W_C}$ in equation (25), $\mathbf{C_C} = \mathbf{W_C^T W_C} + \sigma_C^2\mathbf{I}$. Estimates of λ_C and σ_C^2 are found by maximizing equation (26) using numerical optimization [*Nocedal and Wright*, 2006] with the constraint that λ_C and σ_C^2 are positive. The corresponding MAD is then given by the following:

$$\mathrm{MAD_C} = \arctan\left(\sqrt{\frac{2\sigma_C^2}{\lambda_C}}\right). \tag{27}$$

This PPCA solution is referred to here as a *constrained* fit to avoid confusion with anchored fits. With respect to the BIC, the number of unknowns estimated in the constrained fit is 5 (the mean contains three unknowns, plus λ_C and σ_C^2). This enables Bayesian model selection comparing two hypotheses as follows.

1. H_U: The demagnetization data are realizations drawn from the Gaussian distribution $\mathcal{N}(\boldsymbol{\mu}, \mathbf{C})$, where $\mathbf{C}$ is based on the unanchored PPCA solution.
2. H_C: The demagnetization data are realizations drawn from the Gaussian distribution $\mathcal{N}(\boldsymbol{\mu}, \mathbf{W_C^T W_C} + \sigma_C^2\mathbf{I})$ based on a constrained PPCA solution.

Using the same approach as outlined in section 3.2, $p(H_C|D)$ can be estimated using the BIC approximation to BF.

The example shown in Figure 2 is reexamined using a constrained fit (Figure 4). When comparing anchored versus unanchored fits, the data yield $p(H_A|D) = 0.001$, which indicates very strong support for an unanchored fit. This lack of support for anchoring results from the inappropriateness of $\mathbf{S_A}$ to represent the data. In contrast, when considering a constrained versus unanchored fit, $p(H_C|D) = 0.82$, which indicates that there is positive support for a constrained fit (see Table 2). In addition, the covariance structure of the constrained fit is not spuriously elongated (compare Figure 4b to Figure 2b) and, therefore, does not lead to an artificial reduction in MAD (MAD = 7.5°, $\mathrm{MAD_A} = 2.5°$, and $\mathrm{MAD_C} = 8.3°$). The result $\mathrm{MAD_C} > \mathrm{MAD}$ makes intuitive sense. To accommodate a fit that passes through the origin, the Gaussian distribution that represents the constrained fit must be slightly more rounded than the unanchored fit; therefore, the directional uncertainty must increase. This contrasts with the paradox of $\mathrm{MAD_A}$, where decreasing the agreement between the data and the fitted direction can result in a decreased level of uncertainty associated with that direction.

To further demonstrate constrained fitting, we refer to the examples from *Johnson et al.* [1998] given in section 3.3. Specimens az13b2, az23a1, az26j2, and az12e1 yield $p(H_C|D)$ values of 0.88, 0.91, 0.66, and 0.00, respectively (Figure 5). This indicates that there is positive support for selecting a constrained fit over an unanchored fit for specimens az13b2 and az23a1, weak support for a constrained fit for specimen az26j2, and no support for a constrain fit for specimen az12e1. Thus, use of a constrained fit will produce a remanence direction that passes through the origin without the covariance elongation that made anchoring statistically untenable (Figure 3). For all of the data shown in Figure 5, $\mathrm{MAD_C} \geq \mathrm{MAD}$, which corresponds to increased directional uncertainty as the fitted model rotates away from the data and toward the origin. Thus, our proposed constrained PPCA approach resolves a longstanding problem associated with calculation of MAD values from the standard PCA approach of *Kirschvink* [1980].

5. Conclusions

Anchoring of hypothesized ChRM components can have a strong influence on the estimated paleomagnetic direction and associated uncertainty. If anchoring is to be justified, the resulting PCA fit must be consistent with the demagnetization data. We employ a Bayesian model selection technique to estimate the relative support provided by demagnetization data to unanchored and anchored PCA fits. Importantly, this approach considers anchoring-induced changes in both the paleomagnetic direction and its associated uncertainty, rather than considering the direction alone. We recommend that when anchored fits are used, researchers should also quote $p(H_A|D)$ and its corresponding grade of support (Table 1). Similarly, paleomagnetic directions reconstructed from long sediment cores could be accompanied with a plot of $p(H_A|D)$ versus depth (in addition to MAD or $\mathrm{MAD_A}$ values as appropriate) to demonstrate whether anchoring is justified throughout the core.

The anchoring approach of *Kirschvink* [1980] can lead to spurious elongation of the PCA covariance structure, which in turn artificially reduces directional uncertainty. This property means that anchoring often cannot be supported from a statistical standpoint even when demagnetization data are clearly directed toward the origin of a vector demagnetization diagram. To remedy this inconsistency, we present a new PPCA-based technique to fit vectors that are constrained to pass through the vector demagnetization diagram origin. This approach reduces the level of distortion in the model covariance structure and, thus, provides more realistic ChRM vector determinations. In addition, constrained fitting removes the artificial reduction in MAD associated with the covariance elongation induced by anchoring and provides a more rigorous assessment of directional uncertainty. As with anchoring, if investigators wish to employ a constrained fit, it is crucial to state MAD_C and to justify the decision to adopt a constrained fit by quoting $p(H_C|D)$ and the corresponding grade of support (Table 2).

Acknowledgments
This work was supported by the Australian Research Council (grant DP120103952). The authors are grateful to Lisa Tauxe and Cor Langereis for their constructive comments that improved the manuscript. An Excel Workbook that can be used to perform all of the discussed calculations is available from the authors or can be downloaded from https://dl.dropboxusercontent.com/u/87557845/PPCA/PPCA.zip.

References

As, J. A., and J. D. A. Zijderveld (1958), Magnetic cleaning of rocks in palaeomagnetic research, *Geophys. J. R. Astron. Soc.*, *1*, 308–319.
Bayes, T. (1763), An essay towards solving a problem in the doctrine of chances, *Philos. Trans.*, *53*, 370–418.
Channell, J. E. T., C. Ohneiser, Y. Yamamoto, and M. S. Kesler (2013), Oligocene-Miocene magnetic stratigraphy carried by biogenic magnetite at sites U1334 and U1335 (equatorial Pacific Ocean), *Geochem. Geophys. Geosyst.*, *14*, 265–282, doi:10.1029/2012GC004429.
Collinson, D. W., K. M. Creer, and S. K. Runcorn (1967), *Methods in Palaeomagnetism*, 609 pp., Elsevier, Amsterdam.
Dunlop, D. J. (1979), On the use of Zijderveld vector diagrams in multicomponent paleomagnetic studies, *Phys. Earth Planet. Inter.*, *20*, 12–24.
Heslop, D., and A. P. Roberts (2016), Estimation and propagation of uncertainties associated with paleomagnetic directions, *J. Geophys. Res. Solid Earth*, *121*, 2274–2289, doi:10.1002/2015JB012544.
Irving, E. (1964), *Palaeomagnetism and Its Application to Geological and Geophysical Problems*, 399 pp., John Wiley, New York.
Jeffreys, H. (1961), *The Theory of Probability*, 447 pp., Oxford Univ. Press, Oxford, U. K.
Johnson, C. L., J. R. Wijbrans, C. G. Constable, J. Gee, H. Staudigel, L. Tauxe, V.-H. Forjaz, and M. Salgueiro (1998), $^{40}Ar/^{39}Ar$ ages and paleomagnetism of São Miguel lavas, Azores, *Earth Planet. Sci. Lett.*, *160*, 637–649.
Khokhlov, A., and G. Hulot (2016), Principal component analysis of palaeomagnetic directions: Converting a maximum angular deviation (MAD) into an α_{95} angle, *Geophys. J. Int.*, *204*, 274–291.
Kirschvink, J. L. (1980), The least-squares line and plane and the analysis of palaeomagnetic data, *Geophys. J. R. Astron. Soc.*, *62*, 699–718.
Masson, M. E. J. (2011), A tutorial on a practical Bayesian alternative to null-hypothesis significance testing, *Behav. Res.*, *43*, 679–690.
McElhinny, M. W. (1973), *Palaeomagnetism and Plate Tectonics*, 359 pp., Cambridge Univ. Press, Cambridge, U. K.
McElhinny, M. W., and P. L. McFadden (2000), *Paleomagnetism: Continents and Oceans*, 412 pp., Academic Press, San Diego, Calif.
Nocedal, J., and S. Wright (2006), *Numerical Optimization*, 664 pp., Springer, New York.
Pick, T., and L. Tauxe (1993), Holocene paleointensities: Thellier experiments on submarine basaltic glass from the East Pacific Rise, *J. Geophys. Res.*, *98*, 17,949–17,964.
Raftery, A. E. (1995), Bayesian model selection in social research, *Sociol. Methodol.*, *25*, 111–163.
Raftery, A. E. (1999), Bayes factors and BIC: Comment on "A critique of the Bayesian information criterion for model selection", *Socio. Meth. Res.*, *27*, 411–427.
Schwarz, G. E. (1978), Estimating the dimension of a model, *Ann. Stat.*, *6*, 461–464.
Tarling, D. H. (1983), *Palaeomagnetism: Principles and Applications in Geology, Geophysics and Archaeology*, 380 pp., Chapman and Hall, London, U. K.
Tauxe, L., and H. Staudigel (2004), Strength of the geomagnetic field in the Cretaceous Normal Superchron: New data from submarine basaltic glass of the Troodos Ophiolite, *Geochem. Geophys. Geosyst.*, *5*, Q02H06, doi:10.1029/2003GC000635.
Tipping, M. E., and C. M. Bishop (1999), Probabilistic principal component analysis, *J. R. Stat. Soc. B*, *21*, 611–622.
Wagenmakers, E.-J. (2007), A practical solution to the pervasive problems of p values, *Psychon. Bull. Rev.*, *14*, 779–804.
Zijderveld, J. D. A. (1967), A.C. demagnetization of rocks: Analysis of results, in *Methods in Palaeomagnetism*, edited by D. W. Collinson, K. M. Creer, and S. K. Runcorn, pp. 254–286, Elsevier, Amsterdam.